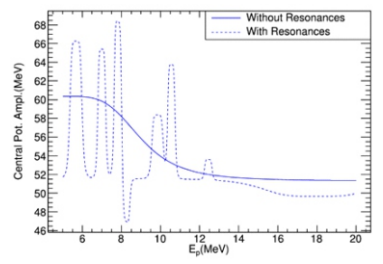
## नाभिकीय अभिक्रिया



# अप्रत्यास्थ प्रकीर्णन अभिक्रियाओं के माध्यम से न्यूक्लिऑन-नाभिक अंतःक्रिया की जांच

## आई. मजुमदार

नाभिकीय एवं परमाणु विज्ञान विभाग, टाटा मुलभृत अन्वेषण संस्थान, होमी भाभा मार्ग, मुंबई-400005, भारत



अनुनाद सहित एवं रहित आपतित प्रोटॉन ऊर्जा के साथ केंद्रीय-संभावित अवधि के

आयाम में अंतर

#### सारांश

इस आलेख में, हम 8-16 MeV की प्रोटॉन ऊर्जा हेतु <sup>16</sup>O(p,p'ү)<sup>16</sup>O अभिक्रिया से 6.13, 6.92 एवं  $7.12~{
m MeV}$   $\gamma$ -किरणों के पूर्ण उत्पादन अनुप्रस्थ काट की रिपोर्ट करते हैं। तीन  $\gamma$ -किरणों के कोणीय वितरण को 9 MeV पर सात कोणों से मापा गया। अनुप्रस्थ काट आकड़ों का विश्लेषण करने के लिए एक विस्तृत फेनोमेनोलॉजिकल ऑप्टिकल मॉडल पोटेंशिँयल (ओ. एम. पी.) स्थापित किया गया। 16O की निचली स्थितियों को जोड़ा गया और विरूपण मापदंडों का उपयोग करके ऑप्टिकल क्षमता को विकृत किया गया। नाभिकीय संरचना प्रभावों की गणना के लिए अनेक अनुनाद शामिल किए गए। आंकड़े के साथ गणनाओं की तुलना चैनल युग्मन, p+160 प्रणाली में अनुनाद एवं प्रक्षेप्य ऊर्जा के साथ अनुदैरध्य-काट की भिन्नता में लक्ष्य विरूपण की जटिल भूमिकाओं को प्रकट करती है।

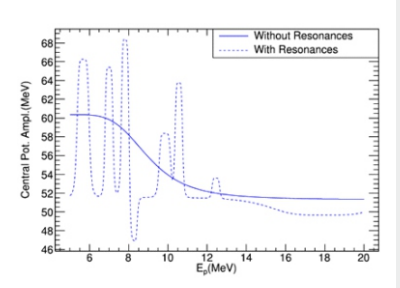
## **Nuclear Reactions**



# Probing Nucleon-Nucleus Interaction through Inelastic Scattering Reactions

## I. Mazumdar

<sup>1</sup>Department of Nuclear and Atomic Physics, Tata Institute of Fundamental Research, Homi Bhabha Road, Mumbai-400005, INDIA



Variation of the amplitude of centralpotential term with incident proton energy, with and without resonances.

#### **ABSTRACT**

In this article, we report the absolute production cross-section of 6.13, 6.92 and 7.12 MeV  $\gamma$ -rays from the  $^{16}\text{O}(p,~p'\gamma)^{16}\text{O}$  reaction for proton energy of 8-16 MeV. Angular distributions of the three  $\gamma$ -rays have been measured for seven angles at 9 MeV. A detailed phenomenological optical model potential (OMP) was set up to analyze the cross-section data. Low-lying states of  $^{16}$ O were coupled and the optical potential was deformed using deformation parameters. Several resonances were included in the calculations to account for the nuclear structure effects. The comparisons of the calculations with the data bring forth the rather complex roles of channel couplings, resonances in the p+160 system and target deformation in the variation of the cross sections with projectile energy.

KEYWORDS: Optical model potential, Nuclear reactions, γ-ray cross-section

<sup>\*</sup>Author for Correspondence: I. Mazumdar F-mail: indra@tifr.res.in

#### Introduction

Notwithstanding the overarching role of heavy-ion-induced reactions in nuclear physics, light-ion-induced reactions continue to have their own importance. A variety of light-ioninduced reactions, namely, elastic and inelastic scattering, capture, charge exchange, knock-out etc, are essential to probe the quantum structure of low-lying states, reaction dynamics and nucleon-nucleus interactions. Nucleon-nucleus (NA) scattering plays a significant role in studying how nucleonnucleon (NN) interaction dynamics and the structure of the target nucleus can give rise to complicated many-body NA scattering. Furthermore, the knowledge of NA scattering can be used to understand nucleus-nucleus (AA) scattering as a superposition of corresponding NA interactions [1]. Apart from the nuclear structure point of view, NA scattering measurements for light nuclei are also valuable for y-ray astronomy [2]. Guided by these objectives, our group has completed a series of measurements to study the low-lying states of light nuclei such as <sup>12</sup>C, <sup>16</sup>O, <sup>10,11</sup>B for insights into the nuclear structure and to contribute towards γ-ray astronomy [3,4]. It is worth mentioning that we have also measured alpha particle-induced scattering cross sections for comparative studies of isospin dependence of nucleon-nucleus interaction. In this brief report we discuss our measurements and theoretical analysis of  $160(p,p'\gamma)^{16}0$  reaction as a representative case of the larger body of work [5].

The primary aim of this work is to measure the angular distributions and absolute production cross-sections of the three low-lying transitions, namely, 6.13, 6.92 and 7.12 MeV. Fig.1 shows the partial level scheme of these low-lying transitions of <sup>16</sup>O [6]. In the energy range of 8-16 MeV, only three groups (Dyer et al. [7], Boromiza et al. [8], Kiener et al. [9]) have reported production cross-sections of these transitions. However, owing to the thick target used by Boromiza et al, the uncertainty in proton beam interaction energy was quite large. This becomes problematic in low-energy regions where there are several resonances. Moreover, the cross-section for 6.92 MeV γ-ray was not reported. The cross sections reported in [9] were normalised to previous measurements of Dyer et al [7] instead of absolute measurements. The absolute cross sections of 6.92 MeV have not been reported so far.

We have attempted to measure the angular distributions and absolute cross sections of all these three transitions. The measured cross sections have been compared with our calculations using optical model potentials (OMPs) within the framework of coupled channel analysis and including several resonances for the p+160 system. We have generated the OMPs from global fits to a large body of experimental data available in the literature. The potentials so generated, have been used to calculate the total and differential angular distribution cross sections for both  $^{16}O(p,p')^{16}O$  and  $^{16}O(p,p'\gamma)^{16}O$  reactions. The comparisons of the calculations with the data bring forth the rather complex roles of target deformation, channel couplings and resonances in the p+160 system.

#### Experimental Details

The experiment was performed at the TIFR-BARC Pelletron facility at TIFR, Mumbai. Self-supporting Mylar target of thickness 2.22 mg cm<sup>-2</sup> was bombarded with protons at 15 beam energies from 8 to 16 MeV. The y-rays were detected by a large volume 3.5"×6" cylindrical Lanthanum Bromide detector. This large volume detector has been thoroughly characterised for y-rays of energy ranging from a few hundred keV to 22.5 MeV [10]. The detector was placed at angles of  $45^{\circ}$ ,  $60^{\circ}$ , 75°, 90°, 105°, 120°, and 135° with respect to the beam direction for angular distribution measurements. Fig.2 presents a typical gamma-ray spectrum measured by the large volume detector at proton beam energy of 10 MeV. One of the crucial aspects of the data reduction and extraction of the absolute cross section is the accurate estimation of the background. The background is created by the tails of the multiple gamma rays and ambient radioactivity. We have tried to generate the background by rigorous Monte Carlo calculations using the GEANT4 package. The spectral shapes for a host of gamma rays produced from the reaction have been generated by the GEANT4. The GEANT4 generated background is shown in Fig.2. The absolute production cross sections of the three transitions were extracted from the efficiency corrected yields for all the beam energies. A fuller description of the theoretical analysis and reproduction of the measured cross sections are provided in the following section.

#### Theoretical Analysis

Optical model analysis has played a central role in nuclear reaction studies. The OMP can successfully explain the scattering of the nucleon from medium to heavy mass (A > 40) target nuclei and at high incident projectile energy (> 40 MeV). However, this formalism has only been reasonably successful for low mass nuclei bombarded by low energy projectiles [11, 12]. There have been instances when the conventional parameterisation of OMP has been found inadequate in describing the elastic scattering data for light target nuclei. The cause of these inadequacies has been assigned to resonances in the compound nucleus, limitations of Woods Saxon form factor, coupling of various channels, giant resonances, etc [13]. The  $^{16}O(p,p'\gamma)^{16}O$  scattering can be modelled as a two-step process; first, the excitation, followed by the de-excitation of the oxygen nucleus. The formal development of the theoretical optical potential allows for a clean separation between the elastic and inelastic channels and the relation between the two [14].

In essence, it is assumed in an optical model that if the elastic and the total reaction channels are well understood (Optical Theorem), then the other channels are mere details. The interaction of a nucleus with a proton projectile of energy in the 5-20MeV range poses challenges to theorists, even if only to describe the elastic scattering channel. To circumvent much

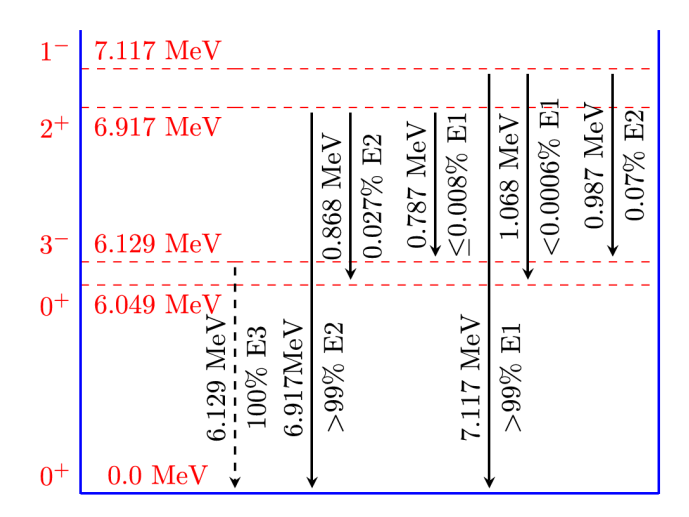


Fig.1: Partial level scheme of 160.

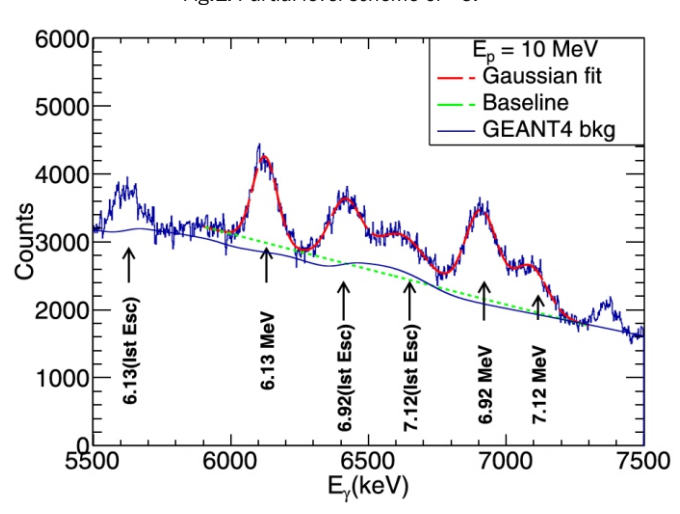


Fig.2: A typical measured y-ray spectrum. Different full energy peaks from de-excitation of  $^{16}$ O nuclei and the corresponding 1st escape peaks are labelled. The overall smooth Compton background under the peaks used in the multi-peak fittings is shown by the dotted green line. The GEANT4 simulated background is shown by the solid blue line.

of the theoretical challenge of this energy region, one can use phenomenological optical potentials, which are blatantly fit to the elastic scattering data. The trade-off for a good quality fit to the elastic channel data is a lack of physical insight. Microscopic notions of anti-symmetry, Pauli blocking, nucleon degrees of freedom, resonances, and nuclear matter properties all get absorbed into this macroscopic 'cloudy ball'. The quality of the fits improves with increase in the number of parameters. Several intertwined steps are involved in calculating the cross-section, such as setting up the OMP, optimizing parameters, inclusion of resonances and deformations, coupling of channels, etc. These steps work simultaneously, rather than sequentially, to provide final cross-section values.

As mentioned in the introductory part we have generated the OMP for the reaction by fitting a large body of global data of elastic scattering, angular distributions, analysing powers etc.

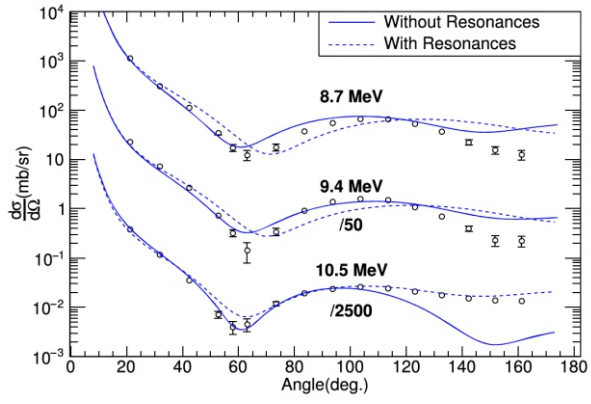


Fig. 3: Optical Model fits to the elastic scattering data available in literature.

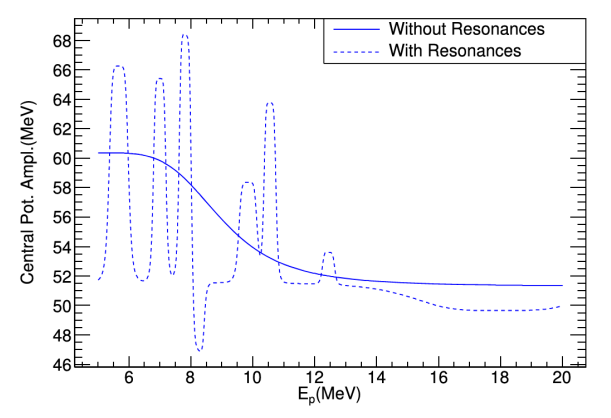


Fig.4: Variation of the amplitude of central-potential term with incident proton energy with and without resonances.

Fig.3 shows the fits to the elastic scattering angular distributions for  $^{16}\text{O}(p,\ p)^{16}\text{O}$  reaction. The effect of nuclear structure on the scattering process manifest through nuclear deformation, coupling of states and inclusion of resonances in the p+ $^{16}\text{O}$  system. The macroscopic, phenomenological optical model is a good doorway to describe inelastic scattering considering collective nuclear excitation, namely, vibration and rotation. These vibration and rotation models have successfully described excitation bands in heavier nuclei. It assumes that the nucleus is non-spherical and has multi-pole deformations that are either causing an excited rotation and/or vibrational mode. It starts by expanding the radius, assuming a series of deformations.

$$R(\theta) = R_0 [1 + \beta_2 Y_2^0(\theta) + \beta_4 Y_4^0(\theta) + \beta_6 2 Y_6^0(\theta) + \dots]$$

Where  $\beta i$ 's are deformation parameters. In a rotational model, these are corresponding to quadrupole, octupole, and hexadecapole rotational modes, whereby symmetry, of only even modes are allowed [15, 1]. There is a partial wave-dependent asymmetry in the polar angle separating  $\vec{r}$  and  $\vec{r}$ ' in coordinate space. The same common multi-pole expansion can be performed on the optical potential, with,  $x=\cos(\theta)$ 

 $V_{\lambda}(|\vec{r}|,|\vec{r}'|) = \frac{1}{2} \int_{-1}^{+1} V(\vec{r},\vec{r}',x) P_{\lambda}(x) dx$ 

where R=r̄'-r̄. The rotational bands are very common in heavy nuclei but are rarely used by themselves in the oxygen nucleus, they are usually combined with vibrations. The vibrational mode looks similar:

$$R(\theta) = R_0 \left[ 1 + \sum_{\lambda,\mu} \alpha_{\lambda}^{\mu} \right]$$

where

$$\alpha_{\lambda}^{\mu} = \frac{\beta_{\lambda}^{\mu}}{\sqrt{2\lambda + 1}} \left\{ b_{\lambda,\mu} + (-1)^{\mu} b_{\lambda,-\mu}^{+} \right\}$$

As can be seen the  $\alpha_{_{\lambda}}^{^{\mu}}$  contain deformation parameters  $(\beta_{_{\lambda}}^{^{\mu}})$  and phonon creation  $(b_{_{\lambda,\mu}}^{^{\dagger}})$  and destruction  $(b_{_{\lambda,\mu}})$  operators. With a vibrational mode the phonons can follow all allowed electric and magnetic transitions. One can then expand the potential in a Taylor series to first order as:

$$V(r,R) = V(r,R_0) + \frac{d}{dR_0}V(r,R_0)R_0 \sum_{\lambda,\mu} \alpha^{\mu}_{\lambda} Y^{\mu}_{\lambda}(\theta,\phi)$$

So these phonon excitations are also derived from the non-spherical nature of the nucleus. The vibrational, rotational, and a combination of both models can be calculated by common distorted born approximation codes [16, 17, 18]. These codes take as input an elastic channel optical potential and then place it into the chosen vibrational/rotational mode, as the potential into the Schrödinger equation. In our calculations we have assumed a first order vibrator model and have considered the ground state and six excited states.

Next to the nuclear deformation, other critical features of such calculations are coupling of the channels and inclusion of resonances that emanate from the <sup>17</sup>F compound nucleus. As mentioned earlier, the OMP parameters, extracted from our global fits to existing data, have been used within a coupled channel formalism to calculate the cross sections. The importance and power of coupled channel calculations are, by now, very well established. The specific structures in the crosssection plots appear only with the inclusion of channel couplings. In addition to channel couplings, another important necessity is to consider the role of virtual resonance states in the compound nucleus <sup>17</sup>F. The <sup>16</sup>O nucleus has a significant chance of entering a compound resonance with the projectile, which accentuates the interaction strength, thus raising or lowering the cross-sections of every channel in this energy region. Thus, the optical potential, in the energy range from 5 to 20 MeV, did not always achieve great fits with a smooth function but was augmented with a series of seven resonances consistently. Many of these elastic data resonances are caused by virtual states in <sup>17</sup>F. We provide below the equations for the final optical potential, including these narrow energy resonances. Fig.4 presents variation of the amplitude of central-potential term with incident proton energy with and without resonances.

$$V_{0} = -111.533 - \frac{1.9125(E - 18.000)^{4}}{(E - 18.000)^{4} + 3.000^{4}} + \sum_{i}^{2} \frac{A_{0i}(E - E_{i})^{6}}{(E - E_{i})^{6} + W_{i}^{6}}$$

$$W_{0} = -0.416 + \frac{0.2965(E - 18.934)^{4}}{(E - 18.934)^{4} + 3.1487^{4}}$$

$$V_{S} = 6.4697 + \frac{4.6311(E - 8.4178)^{4}}{(E - 8.4178)^{4} + 4.1768^{4}}$$

$$W = 2.3981 - \frac{5.8619(E - 22.00)^{4}}{(E - 22.00)^{4} + 10.3884^{4}} + \sum_{i}^{7ex} \frac{A_{0i}(E - E_{i})^{6}}{(E - E_{i})^{6} + W_{i}^{6}}$$

$$r_{0} = 0.6748 - \frac{0.055231(E - 17.7335)^{4}}{(E - 17.7335)^{4} + 3.6787^{4}} + \sum_{i}^{7ex} \frac{R_{0i}(E - E_{i})^{6}}{(E - E_{i})^{6} + W_{i}^{6}}$$

$$a_{0} = 0.5431 + \frac{0.196843(E - 5.000)^{4}}{(E - 5.000)^{4} + 16.1121^{4}}$$

$$r_{s} = 1.7125 - \frac{0.083141(E - 16.17)^{4}}{(E - 16.17)^{4} + 3.000^{4}} + \sum_{i}^{7ex} \frac{R_{si}(E - E_{i})^{6}}{(E - E_{i})^{6} + W_{i}^{6}}$$

$$a_{s} = 0.38018 - \frac{0.04292(E - 21.692)^{4}}{(E - 21.692)^{4} + 3.038^{4}}$$

$$V_{so} = 8.67746 - \frac{1.95582(E - 17.777)^{4}}{(E - 17.777)^{4} + 3.000^{4}} + \sum_{i}^{7ex} \frac{R_{soi}(E - E_{i})^{6}}{(E - E_{i})^{6} + W_{i}^{6}}$$

$$w_{so} = -0.01782 - \frac{1.3537(E - 10.381)^{4}}{(E - 10.381)^{4} + 4.707^{4}}$$

$$r_{so} = 0.5538 + \frac{0.31743(E - 20.442)^{4}}{(E - 20.442)^{4} + 3.00^{4}} + \sum_{i}^{7ex} \frac{R_{soi}(E - E_{i})^{6}}{(E - E_{i})^{6} + W_{i}^{6}}$$

$$a_{so} = 0.3440 + \frac{0.11343(E - 6.8494)^{4}}{(E - 6.8494)^{4} + 4.344^{4}}}$$

$$r_{c} = 1.3830 + \frac{0.2713(E - 5.000)^{4}}{(E - 5.000)^{4} + 4.308^{4}}$$

rays and total production cross sections, respectively [5]. Our calculations of the total cross-sections for the three y-rays agree fairly well with the measured values. However, there still exist differences between theory and experiments regarding finer structures in the cross sections. It is observed that the value of the target deformation has a considerable effect on the total cross-sections. In the spirit of our phenomenological calculation, we acknowledge that the sensitivity upon deformation merits further study. The discrepancies that persist in terms of finer structure are very likely due to complex and connected structural effects which are yet to be fully understood. There are subtle roles played by both coupling of the channels and resonances, and what may surmise is that the calculation at these low energies loses much of its predictive power. The conclusion carries the unmistakable stamp of the complexity of the problem. It leaves much scope for further improvement in the calculation.

#### Summary

 $\label{proton} \mbox{Proton induced inelastic scattering reactions are of great} \mbox{importance in probing the quantum structure of low-lying}$ 

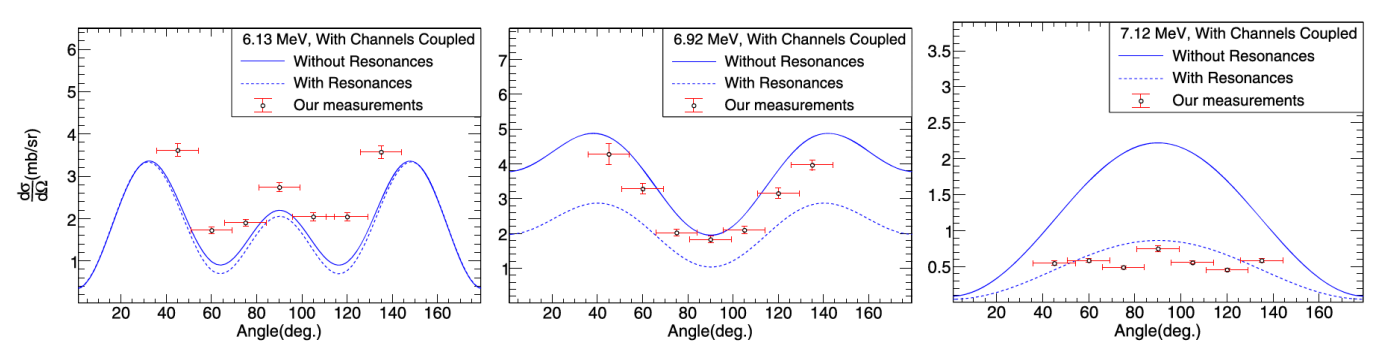


Fig.5: Measured and calculated differential cross-sections for angular distribution of 6.13, 6.92 and 7.12 MeV  $\gamma$ -rays for 9 MeV proton. The coupled channel calculations have been performed with and without resonances.

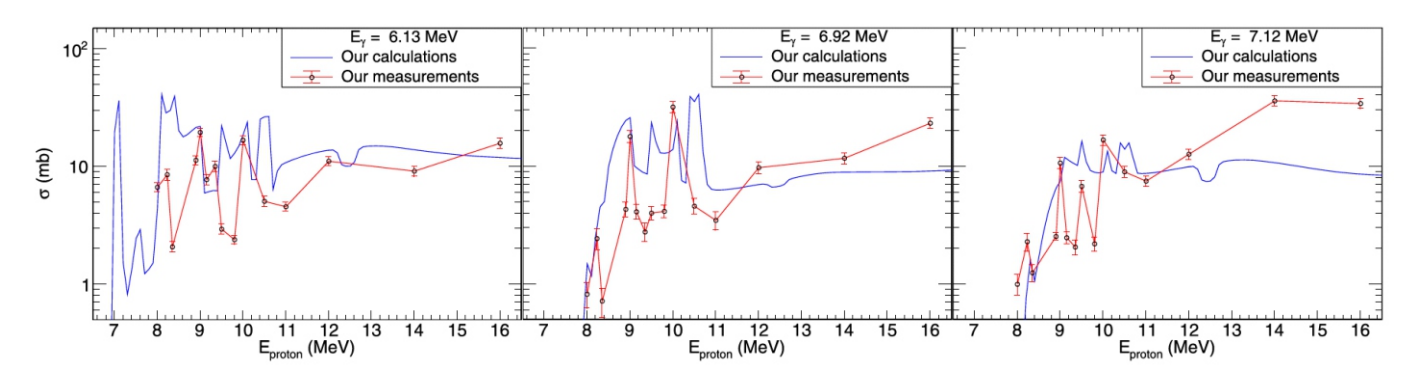


Fig.6: Measured and calculated total cross-sections for production of 6.13, 6.92 and 7.12 MeV γ-rays.

excited states in light nuclei. We have initiated a systematic study of the angular distribution and absolute cross sections of  $(p, p'\gamma)$  reaction on different light nuclei. It is worth noting that unlike (p, p') reaction there are dearth of data for (p, p'γ) reactions from nuclei, like, <sup>12</sup>C, <sup>16</sup>O, <sup>10,11</sup>B etc. On the theoretical side, the reproduction of absolute cross sections from inelastic scattering experiments continues to be a formidable challenge due to the myriad complexities of nuclear structure and reaction mechanisms at low energy and low mass regions. In this report we have presented absolute production cross sections of three transitions in <sup>16</sup>O. The absolute cross section of the 6.92 MeV has been reported for the first time [5]. We have made serious efforts to develop a detailed theoretical analysis package within the framework of Optical Model formalism. The OM potentials have been generated from fits to a large body of global data. The analysis clearly reveals the complexity of the problem and the importance of channel couplings, resonances and nuclear deformations.

#### Acknowledgment

Indranil Mazumdar wishes to thank his collaborators, V. Ranga, S. P. Weppner, R. Sariyal, S. Panwar, A. K. R. Kumar, A. K. Gourishetty, S. M. Patel and P. B. Chavan. He would also like to thank the staff members of the TIFR Pelletron facility for providing the beam for the entire duration of the experiment. DAE is acknowledged for supporting this research work.

#### References

[1] Ray L, Hoffmann G W and Coker WR 1992 Nonrelativistic

- and relativistic descriptions of proton nucleus scattering Phys. Rep. 212, 223–328
- [2] Ramaty R, Kozlovsky B and Lingenfelter R E 1979 Nuclear grays from energetic particle interactions Astrophys. J. Suppl. 40, 487-526
- [3] Mazumdar I, Dhibar M, Weppner S P, Anil Kumar G, Rhine Kumar A K, Patel S M, Chavan P B, Bagdia C D and Tribedi L C 2019 Studies in nuclear structure and big bang nucleosynthesis using proton beams Acta Phys. Polon. B 50, 377
- [4] Dhibar M, Mazumdar I, Anil Kumar G, Weppner S P, Rhine Kumar A K, Patel S M and Chavan P B 2018 Study of 12C(p,p'g)12C reaction arXiv:1806.02126
- [5] V. Ranga, I. Mazumdar, S.P. Weppner, S. Panwar, R. Sariyal, S. M. Patel, P.B. Chavan, A. K. Rhine Kumar and G. Anil Kumar, Measurement of proton induced absolute production cross section of 6.12, 6.92 and 7.12 MeV g-rays from 160(p, p'g)160 reaction, Journal of Physics G: Nucl. Part. Phys. 51 (2024) 045101
- [6] Tilley D R, Weller H R and Cheves C M 1993 Energy levels of light nuclei A = 16-17 Nucl. Phys. A 5641-183
- [7] Dyer P, Bodansky D, Seamster A G, Norman E B and Maxson D R 1981 Cross sections relevant to g-ray astronomy: proton induced reactions Phys. Rev. C 23, 1865
- [8] Boromiza M et al 2020 Nucleon inelastic scattering cross sections on 160 and 28Si Phys. Rev. C 101, 024604
- [9] Kiener J, Berheide M, Achouri N L, Boughrara A, Coc A, Lefebvre A, de Oliveira Santos F and Vieu C 1998 g-ray production

- by inelastic proton scattering on 160 and 12C Phys. Rev. C 58, 2174-9
- [10] Mazumdar I, Gothe D A, Anil Kumar G, Yadav N, Chavan P B and Patel S M 2013 Studying the properties and response of a large volume (946 cm3) LaBr3:Ce detector with g-rays up to 22.5 MeV Nucl. Instrum. Methods Phys. Res., Sect.A 705, 85–92
- [11] Amos K, Dortmans P J, von Geramb H V, Karataglidis S and Raynnal J 2000 Nucleon–Nucleus Scattering: A Microscopic Nonrelativistic Approach (Boston: Springer) pp 276–536
- [12] Weppner S P, Penney R B, Diffendale G W and Vittorini G 2009 Isospin dependent global nucleon–nucleus optical model at intermediate energies Phys. Rev. C 80 034608
- [13] Petler J S, Islam M S, Finlay R W and Dietrich F S 1985 Microscopic optical model analysis of nucleon scattering from light nuclei Phys. Rev. C 32, 673–84

- [14] Watson K M 1953 Multiple scattering and the many-body problem-applications to photomeson production in complex nuclei Phys. Rev. 89, 575–87
- [15] Jelley N A 1990 Fundamentals of Nuclear Physics (Cambridge: Cambridge University Press) chapter 8
- [16] Raynal J 1994 Notes on ECIS94 Technical Report CEA-N-2772, Commisariat 'a l'Energie Atomique, Saclay, France pp 1–145
- [17] Raynal J 2006 ECIS-06.
- http://www.oecd-nea.org/tools/abstract/detail/nea-0850
- [18] Thompson I J 2006 FRESCO. http://www.fresco.org.uk20] S. K. Pandit, A. Shrivastava, K. Mahata, N. Keeley, V. V. Parkar, P. C. Rout, K. Ramachandran, I. Martel, C. S. Palshetkar, A. Kumar, A. Chatterjee, and S. Kailas, Phys. Rev. C 93,061602® (2016).